Slow isocharged sequence ions with helium collisions: Projectile core dependence

Deyang Yu,[1,*] Xiaohong Cai,[1,†] Rongchun Lu,[1,2] Fangfang Ruan,[1,2] Caojie Shao,[1] Hongqiang Zhang,[3] Ying Cui,[3] Jun Lu,[1] Xu Xu,[3] Jianxiong Shao,[3] Baowei Ding,[3] Zhihu Yang,[1] Ximeng Chen,[3] and Zhaoyuan Liu[3]

[1]*Institute of Modern Physics, Chinese Academy of Sciences, Lanzhou 730000, People's Republic of China*

[2]*Graduate School of the Chinese Academy of Sciences, Beijing 100049, People's Republic of China*

[3]*Department of Modern Physics, Lanzhou University, Lanzhou 730000, People's Republic of China*

(Received 11 January 2007; published 22 August 2007)

The collisions of the isocharged sequence ions of $q=6$ (C^{6+}, N^{6+}, O^{6+}, F^{6+}, Ne^{6+}, Ar^{6+}, and Ca^{6+}), $q=7$ (F^{7+}, Ne^{7+}, S^{7+}, Ar^{7+}, and Ca^{7+}), $q=8$ (F^{8+}, Ne^{8+}, Ar^{8+}, and Ca^{8+}), $q=9$ (F^{9+}, Ne^{9+}, Si^{9+}, S^{9+}, Ar^{9+}, and Ca^{9+}) and $q=11$ (Si^{11+}, Ar^{11+}, and Ca^{11+}) with helium at the same velocities were investigated. The cross-section ratios of the double-electron transfer (DET) to the single-electron capture (SEC) $\sigma^{DET}/\sigma^{SEC}$ and the *true* double-electron capture (TDC) to the double-electron transfer $\sigma^{TDC}/\sigma^{DET}$ were measured. It shows that for different ions in an isocharged sequence, the experimental cross-section ratio $\sigma^{DET}/\sigma^{SEC}$ varies by a factor of 3. The results confirm that the *projectile core* is another dominant factor besides the *charge state* and the *collision velocity* in slow ($0.35-0.49v_0$; v_0 denotes the Bohr velocity) highly charged ions (HCIs) with helium collisions. The experimental cross-section ratio $\sigma^{DET}/\sigma^{SEC}$ is compared with the extended classical over-barrier model (ECBM) [A. Bárány *et al.*, Nucl. Instrum. Methods Phys. Res. B **9**, 397 (1985)], the molecular Coulombic barrier model (MCBM) [A. Niehaus, J. Phys. B **19**, 2925 (1986)], and the semiempirical scaling laws (SSL) [N. Selberg *et al.*, Phys. Rev. A **54**, 4127 (1996)]. It also shows that the projectile core properties affect the initial capture probabilities as well as the subsequent relaxation of the projectiles. The experimental cross-section ratio $\sigma^{TDC}/\sigma^{DET}$ for those lower isocharged sequences is dramatically affected by the projectile core structure, while for those sufficiently highly isocharged sequences, the autoionization always dominates, hence the cross-section ratio $\sigma^{TDC}/\sigma^{DET}$ is always small.

DOI: 10.1103/PhysRevA.76.022710 PACS number(s): 34.70.+e, 82.30.Fi

I. INTRODUCTION

In the past several decades the study of ion-atom collisions is demanded and stimulated by applied physics such as controlled fusion research as well as astrophysics. Moreover, it is also interesting because it provides instances of many-body collision dynamics of pure electromagnetic system governed by quantum rules.

The single-electron transfer process in ion-atom collisions is understood quite well at keV energies [1,2]. Owing to more open channels, the collision dynamics of the double-electron processes are much more complicated. Since the advent of the electron cyclotron resonance ion source (ECRIS) and the electron beam ion source (EBIS) in the 1980s, the research of multielectron processes in low energy HCI-atom collisions has been greatly promoted. The early knowledge and the experimental results on HCI-atom collisions were reviewed by Janev and Presnyakov [3] and by Barat and Roncin [4]. The cross sections of the SEC, the DET, and the TI process by highly stripped ($2\leq q\leq 13$), slow ($0.25q$ keV and $1q$ keV) Ne^{q+}, Ar^{q+}, Kr^{q+}, and Xe^{q+} ions on helium collisions were reported by Justiniano *et al.* [5]. They pointed out that the DET (including the TI and the TDC) process is typically an order of magnitude weaker than the SEC process, and dominated by the TI channel in most cases. The absolute cross sections σ^{SEC} and σ^{TI} are measured by Andersson *et al.* [6] in Xe^{q+}-He ($11\leq q\leq 31$) collisions at $4q$ keV, and their results also show that the TDC is much weaker than the TI. The single- and double-electron capture cross sections in Ar^{q+}-He ($8\leq q\leq 16$) collisions at $2.3q$ keV were measured by Vancura *et al.* [7]. By means of the translational energy-gain method, Cederquist *et al.* [8] studied the electron population in Ar^{q+}-He ($15\leq q\leq 18$) collisions. Cederquist *et al.* [9,10] also measured the mean Q values of the SEC and the TI channels in slow collisions between very highly charged Xe^{q+} ($25\leq q\leq 44$) and helium atoms. They argued that the transfer excitation (TE) process is an important channel in slow HCI-helium collisions. Fléchard *et al.* [11] studied the single- and the double-electron capture processes in Ne^{10+} with helium collisions in the energy region of 50–150 keV. The total and differential cross sections of state selection were obtained, and the results are in good agreement with the semiclassical close-coupling calculations. Bliman *et al.* [12] studied the Ar^{9+}-He collision at 2.25 keV/u by using the XUV-VUV spectroscopy and the Auger spectroscopy complementarily. They identified the optical spectrum as well as the Auger spectrum, and found that the TDC mainly results in Na-like core excited states corresponding to the configurations $1s^22s^22p^53l5l'$. The absolute cross sections σ^{SEC}, σ^{TI}, and σ^{TDC} of Xe^{q+}-He ($30\leq q\leq 42$) collision are measured by Selberg *et al.* [13,14] at $3.8q$ keV. A set of semiempirical scaling laws (SSL) was proposed to estimate the cross sections and the cross-section ratios. Recently, the cross-section ratio $\sigma^{DET}/\sigma^{SEC}$ of Ta^{q+}-He ($41\leq q\leq 49$) collisions at $0.3v_0$ were experimentally investigated by Madzunkov *et al.* [15], and their data show good agreement with SSL proposed by Selberg *et al.* [13].

The DET process was discussed by Janev and Presnyakov [3] in the frame of the Landau-Zener approximation. Fritsch

*d.yu@impcas.ac.cn

†caixh@impcas.ac.cn

and Lin [2,16–18] studied the DET process in slow O^{6+}, C^{6+}, B^{4+}, Be^{4+}, and C^{5+} with helium collisions within the semiclassical close-coupling description. And the DET process in B^{4+}-He collisions was also investigated by Bacchus-Montabonal [19]. In the diabatic molecular representation, Chaudhuri *et al.* [20] investigated double-electron processes in , collisions. A theoretical study on the DET process in 1–50 keV He^{2+}-He collisions was done by Tergiman and Bacchus-Montabonal [21]. In addition, the shake-off mechanism was also introduced into slow HCI-atom collisions [22]. However, because of the complexity originated from many active electrons which are involved during the HCI-atom interaction, the full quantum treatment is rather difficult. Therefore, the simple classical over-the-barrier models [23–25] and the semiempirical scaling laws [13,26] are widely employed to obtain intuitional pictures as well as to compare with experimental results. The projectile core properties are always entirely neglected in these classical models and in the semiempirical scaling laws since they describe the projectile ions only by their charge state q, thus they are not able to distinguish the different ions in an isocharged sequence.

Although the collisions of HCI with atoms at low energies have been widely studied [4] and in great detail [27], the projectile core dependence character of the DET process in HCI-He collisions is still far from being fairly understood [11,28–30], and the firsthand experimental data, especially for those concentrating on isocharged sequence ions, are still very scarce. By means of VUV spectroscopy, Dijkkamp *et al.* [31] measured the subshell-selective SEC cross sections of C^{6+}, N^{6+}, O^{6+}, and Ne^{6+} with helium and C^{6+}, N^{6+}, and O^{6+} with argon collisions in the velocity range 0.15–0.5 au. They found that the structure of the projectile core is not very important for the l distribution. But later similar work of C^{6+}, O^{6+}, and Ne^{6+}-He collisions at lower velocities (0.05–0.27 au.) by Beijers *et al.* [32,33] shows visible projectile core effects on the SEC process. Nijs *et al.* [34] measured the charge-state distribution of the target ions produced in collisions of C^{6+}, N^{6+}, O^{6+}, Ne^{6+}, Ar^{6+}, and Kr^{6+} on argon at keV energies. An obvious difference was observed between the light ions C^{6+}, N^{6+} and the heavy ions Ar^{6+}, Kr^{6+}. Our previous works on isocharged ions with neon [35] and argon [36] collisions also show projectile core effects. The collisions of Ar^{16+}, Kr^{16+}, and Xe^{16+} with C_{60} at $0.28v_0$ were studied by Bernard *et al.* [37]. They found that the core effect is rather small for this high charge state, and it only appears when the number of the transferred electrons is sufficiently high.

The aim of this work is to experimentally examine the projectile core dependence in slow HCI-atom collisions. In this paper, we report systematic experimental study of slow collisions between isocharged ions and helium at the same velocities. In the following section, we will describe the classical over-the-barrier models and the semiempirical scaling laws, and then the experimental setup and the measuring procedures will be presented in Sec. III. The results and discussion are presented in Sec. IV and Sec. V is the conclusions.

II. CLASSICAL OVER-THE-BARRIER MODELS AND THE SEMIEMPIRICAL SCALING LAWS

The prototype of the classical over-the-barrier model was introduced by Bohr and Lindhardt [38] for the single-electron atom, and then it was elaborated by Kundsen *et al.* [23]. According to this model, the SEC cross section of slow (keV/u) ion-atom collision is proportional with the projectile charge state q but independent of any other factors. This idea was applied to multielectron atoms by Ryufuku *et al.* [39], and soon was extended by Bárány *et al.* [24] and by Niehaus [25]. In principle, the classical over-the-barrier models treat the ion-atom interaction as a process of the Coulomb potential barrier falling and raising, and therefore the electrons repopulate between the projectile and the target. The most sophisticated model is known as MCBM proposed by Niehaus [25], which distinguishes the closing (*way in*) and separating (*way out*) periods of the two nuclei, and estimates the transfer probabilities of the electrons. A critical experimental examination of MCBM was performed by Guillemot *et al.* [40] with argon and xenon atoms as the target. ECBM was also experimentally examined by Nakamura *et al.* [41] with Ne, Ar, Kr, and Xe as the target.

It is well known that the cross sections are quite large in slow HCI-He collisions, even the DET cross sections can be as large as 10^{-15} cm^2 [14]. This implies that the collision parameter is ordinarily quite big and hence the deflection of the projectile trajectory as well as the energy loss are small. In fact, it is usually considered that the projectiles pass by the target atoms rectilinearly with uniform velocities. Therefore, the mass of the projectile ions is usually considered not affecting the electrons transfer mechanism. In addition, for sufficiently highly charged partially stripped ions, the core electrons are usually considered as spectators. As the collision velocity is lower than the classical orbital velocity of the target electrons, the direct ionization (DI) channel is strongly inhibited [4,42]. Thus the only effective channels are the electron-capture processes as well as the TI process due to the subsequent autoionization. In the classical picture, it is usually considered that (1) the motion of the nuclei can be treated as classical trajectories, and usually be simplified as straight lines; (2) the reaction can be divided into two independent stages: the initial electron transfer stage and the projectile relaxation stage; (3) in the initial electron transfer stage, the target electrons are activated in sequence order by their ionization potential, and transferred from the target atom to the projectile ion; and (4) in the projectile relaxation stage, the projectile ions, which can possibly be doubly excited, will deexcite. The photon deexcitation results in the TDC process and the autoionization results in the TI process.

The two electrons of an isolated helium atom are equivalent, i.e., their spatial wave functions are the same. Nevertheless, the two electrons of a helium atom are not independent, and the electron-electron correlation influences the DET process. From a classical point of view, during the helium atom interacting with an HCI, once one electron overcomes the Coulomb barrier with the energy of −24.6 eV (i.e., the first ionization potential), the electron-electron repulsion will disappear, then another electron will fall into the energy level of −54.4 eV (i.e., the second ionization poten-

tial). Therefore, the symmetry between the two electrons will be broken when an electron transfers. So it is reasonable to differentiate the two electrons as "outer" and "inner" by their ionization potential in electron transfer processes during HCI-atom interaction. The DET process following this hypothesis is the so-called two-step mechanism, as taken by the classical over-the-barrier models [24,25,39]. However, if the electron-HCI interaction is much stronger than the electron-electron interaction, the two electrons can also overcome the Coulomb barrier simultaneously with similar energies and be semisymmetrically populated. This is a possible one-step mechanism of the DET process [26].

Starting from their experimental results of slow Xe^{q+} ions ($15 \leq q \leq 43$) colliding with He, Ar, and Xe, Selberg *et al.* [13,14] presented a set of semiempirical scaling laws (SSL) for different electronic rearrangement features in slow HCI-atoms collisions. The cross sections σ_q^r for removing exactly r electrons from the target atom by an HCI with charge state q is formulated as follows [13]:

$$\sigma_q^r = 2.7 \times 10^{-13} qr \Big/ \left[I_1^2 I_r^2 \sum_{j=1}^{N} (j/I_j^2) \right], \qquad (1)$$

where the cross section σ_q^r is in cm^2, I_j is the jth target ionization potential in eV, and N is the number of outer-shell electrons. Comparing with the experimental result, Selberg *et al.* found that this scaling law gives better predictions than ECBM [24], especially for the cross-section ratio $\sigma_q^{DET}/\sigma_q^{SEC}$ of the helium target [14]. However, this scaling law completely ignores any projectile core properties, and it predicts that the cross-section ratio $\sigma_q^{DET}/\sigma_q^{SEC} = \sigma_q^2/\sigma_q^1 = 2(I_1/I_2)^2$ depends only on the target ionization potentials. For helium this constant is 0.41 [14].

The theoretical predictions of the cross sections σ^{SEC}, σ^{DET} and the cross-section ratio $\sigma^{DET}/\sigma^{SEC}$ of MCBM, ECBM, and SSL for $q=6$, 7, 8, 9, and 11 isocharged ions collision with helium are listed in Table I. As mentioned above, these models do not distinguish different ions within an isocharged sequence.

When different ions in an isocharged sequence pass by an atom with the same velocity and collision parameter, they will pass though the same classical trajectory, as pointed out above. In this situation, the only differences are the different projectile-ion cores and the associated electronic structure of the ions. Therefore, there are two possible ways that the collision dynamics can be affected by (1) the excitation of projectile core electrons, and (2) the exact energetic positions of the electronic states that get populated.

TABLE I. Predictions of MCBM, ECBM, and SSL for the $q=6$, 7, 8, 9, and 11 isocharged sequence ions collision with helium. The unit of the cross sections is 10^{-16} cm^2.

Model	MCBM	ECBM	SSL
$q=6$ isocharged sequence			
σ^{SEC}	23.2	22.3	37.7
σ^{DET}	12.4	15.2	15.4
$\sigma^{DET}/\sigma^{SEC}$	0.54	0.68	0.41
$q=7$ isocharged sequence			
σ^{SEC}	25.8	25.1	44.0
σ^{DET}	15.2	17.5	18.0
$\sigma^{DET}/\sigma^{SEC}$	0.59	0.70	0.41
$q=8$ isocharged sequence			
σ^{SEC}	28.5	28.0	50.3
σ^{DET}	17.8	19.8	20.6
$\sigma^{DET}/\sigma^{SEC}$	0.63	0.71	0.41
$q=9$ isocharged sequence			
σ^{SEC}	31.1	30.8	56.6
σ^{DET}	20.3	22.0	23.1
$\sigma^{DET}/\sigma^{SEC}$	0.65	0.71	0.41
$q=11$ isocharged sequence			
σ^{SEC}	36.4	36.4	69.2
σ^{DET}	25.2	26.4	28.3
$\sigma^{DET}/\sigma^{SEC}$	0.69	0.72	0.41

III. EXPERIMENT

The experiment was carried out on the 14.5 GHz ECRIS at the Institute of Modern Physics, Chinese Academy of Sciences. In brief, the ion beams were q/m selected by a dipole magnet and then transported to the experimental terminal via a 5 m pipeline. Before entering the collision chamber, the beams were purified by a 64° coaxial electrostatic capacitor to remove the charge-state impurities induced by the residual vacuum. The beams were collimated by two groups of two-dimensional collimators (about 0.3×0.3 mm), and then collided with a helium beam ejected from a gas jet in the collision chamber. The recoil ions (He^+ and He^{2+}) were extracted by a weak electrostatic field of a time-of-flight (TOF) spectrometer from the collision zone and accelerated, then detected by a microchannel plate detector. The scattered projectile ions passed though a parallel plate capacitor and were deflected by its electrostatic field, and then detected by a position-sensitive microchannel plate (PSMCP) detector. The charge states of the recoiled ions were determined by measuring their TOF differences from the scattered ions. The charge states of the scattered ions were obtained from the positions where they hit on the PSMCP detector. The experimental data were coincidentally recorded in list mode by an MPA-3 multiparameter acquisition system, while the collision events, which did not happen in the collision region, i.e., in the path, were excluded. By means of position-sensitive detection and TOF coincident technique, the reaction channels of the SEC, the TDC, and the TI channel were distinguished; the relative cross sections were obtained.

The isocharged sequence ions of $q=6$ (C^{6+}, N^{6+}, O^{6+}, F^{6+}, Ne^{6+}, Ar^{6+}, and Ca^{6+}), $q=7$ (O^{7+}, F^{7+}, Ne^{7+}, S^{7+}, and Ar^{7+}), $q=8$ (F^{8+}, Ne^{8+}, Ar^{8+}, and Ca^{8+}), $q=9$ (F^{9+}, Ne^{9+}, Si^{9+}, S^{9+}, Ar^{9+}, and Ca^{9+}) and $q=11$ (Si^{11+}, Ar^{11+}, and Ca^{11+}) were employed to collide on helium atoms. Limited by the acceleration voltage region of the ECRIS, the ion velocities in the $q=6$ and the $q=7$ isocharged sequences were difficult to set to a same value for the lightest and the heaviest ions. In this

situation, we measured the lighter ions (C^{6+}, N^{6+}, and O^{6+}) at a faster velocity ($0.49v_0$, i.e., 6 keV/u) and the heavier ions (Ar^{6+} and Ca^{6+}) at a slower velocity ($0.35v_0$, i.e., 3 keV/u), and the middle ions (F^{6+} and Ne^{6+}) at both velocities. Therefore, one can get information about this velocity difference. In the $q=7$ isocharged sequence, the velocity of F^{7+}, Ne^{7+}, and S^{7+} was $0.43v_0$ (4.67 keV/u), but for Ar^{7+} and Ca^{7+}, they were slightly slower, i.e., $0.42v_0$ (4.38 keV/u) and $0.4v_0$ (4 keV/u), respectively. The velocities of $q=8$, $q=9$, and $q=11$ isocharged sequence ions were $0.4v_0$ (4 keV/u), $0.42v_0$ (4.5 keV/u), and $0.47v_0$ (5.5 keV/u), respectively. To test the reproducibility of the system, the F^{8+}-, Ar^{9+}-, and Ar^{11+}-He collisions were measured two or three times during the experiment. With isotope purified $^{13}CO_2$ as the working gas, the $^{13}C^{6+}$ ion beam was obtained to avoid the mixing with H_2^+ and He^{2+}, etc., which have $q/m=1/2$.

The main experimental uncertainties come from the statistical error of the TDC process, the efficiency difference of the PSMCP detector, and the uncertainty of the counting region in the two-dimension spectrum. The statistical error is rather small for the SEC and the TI channel, and it is typically less than ±10% for the TDC channel. The uniformity of the MCP detector was tested both by an ^{241}Am 5.638 MeV α source and by a 144 keV Ar^{12+} beam from the ECRIS, and the difference of the detection efficiency is within ±10%. The uncertainty of determining the counting region in the two-dimension spectrum is typically less than ±10%. The recoiled He^+ and He^{2+} ions were accelerated by a 2–3 kV electrostatic field before arriving at a circular MCP detector with a 36 mm diameter. Due to this sufficiently high acceleration voltage, the detection efficiency of the recoil ions (i.e., He^+ and He^{2+}) is close to unity, and the efficiency difference between He^+ and He^{2+} is neglectable.

We define it as a multicollision event if a projectile ion interacts with two or more atoms either in the collision region or in the path and therefore changed its charge state. The probability of multicollision can be estimated as follows: supposing the probability of a projectile ion interacting with one atom is p, then the probability of interacting with two atoms is approximately p^2, and the more collisions could be ignored. Thus the ratio between the double- and the single-collision events is $p^2:p=p:1$, which approximately equals the ratio between the single-collision events and the primary projectile ions. In the present work, the target gas flow was controlled by a system of an INFICON VDE016 valve, a TPR265 barometer, and a VCC500 controller. The flow is controlled under 3×10^{-3} mbar L/s, and the total charge-state-changing probability is 1–3%. Therefore, the ratio of the multicollision to the single-collision events is 1–3%.

IV. RESULTS AND DISCUSSION

In slow (keV/u) HCI-He collisions, the SEC process is the primary channel. On the contrary, the DI process is extremely weak and was not observed in the present work. Both the TDC and the TI channels are the consequences during the projectile relaxation after the DET occurs, i.e., $\sigma^{DET}=\sigma^{TDC}+\sigma^{TI}$. It is well known that in the SEC process, the two electrons of a helium atom can also be activated simultaneously, i.e., the transfer excitation (TE) process [10,43–47]

$$\text{SEC:}\quad X^{q+}+He\rightarrow X^{(q-1)+}+He^{+}, \tag{2}$$

$$\text{TE:}\quad X^{q+}+He\rightarrow X^{(q-1)+}+He^{+*}, \tag{3}$$

$$\text{TDC:}\quad X^{q+}+He\rightarrow X^{(q-2)+*}+He^{2+}\rightarrow X^{(q-2)+}+He^{2+}+\gamma, \tag{4}$$

$$\text{TI:}\quad X^{q+}+He\rightarrow X^{(q-2)+*}+He^{2+}\rightarrow X^{(q-1)+}+He^{2+}+e. \tag{5}$$

The autoionization results in the TI channel and the radiative deexcitation results in the TDC channel. The SEC, the TDC, and the TI channels were distinguished in the present experiment. However, the TE channel could not be distinguished from the SEC channel in this work. The cross-section ratios $\sigma^{DET}/\sigma^{SEC}$ and $\sigma^{TDC}/\sigma^{DET}$ were obtained in the present work, and the experimental results are listed in Table II. The initial electron transfer will be discussed in Sec. IV A and the subsequent projectile relaxation will be discussed in Sec. IV B.

A. Initial electron transfer

The cross-section ratio $\sigma^{DET}/\sigma^{SEC}$ of $q=6$ isocharged sequence ions with helium collisions is shown in Fig. 1. As mentioned above, the velocity of C^{6+}, N^{6+}, and O^{6+} is $0.49v_0$ (6 keV/u), the velocity of Ar^{6+} and Ca^{6+} is $0.35v_0$ (3 keV/u). To test the influence of the different velocities, F^{6+} and Ne^{6+} are measured at both velocities. It shows that the effect of different velocities is within the experimental uncertainties. The collision velocity is unimportant in present cases, which is consistent with the experimental facts [4,48,49]. For C^{6+}, N^{6+}, O^{6+}, F^{6+}, and Ne^{6+}, the value of $\sigma^{DET}/\sigma^{SEC}$ is around 0.04–0.09. However, for Ar^{6+}, this value is as high as 0.31, and for Ca^{6+} it is about 0.12. The arithmetic average of all above experimental data is about 0.1, which is also illustrated in Fig. 1. As listed in Table I, MCBM, ECBM, and SSL predict constants of 0.54, 0.68, and 0.41 for the $q=6$ isocharged sequence ions, respectively. The cross-section ratio $\sigma^{DET}/\sigma^{SEC}$ of the $q=7$ isocharged sequence ions F^{7+}, Ne^{7+}, S^{7+}, Ar^{7+}, and Ca^{7+} collision with helium at $0.43v_0$ is illustrated in Fig. 2. It shows that the value varies from 0.19 (Ca^{7+}) to about 0.36 (S^{7+}) and the arithmetic average of these data is about 0.34. As listed in Table I, the predictions of MCBM, ECBM, and SSL are 0.59, 0.70, and 0.41, respectively. Figure 3 gives the cross-section ratios $\sigma^{DET}/\sigma^{SEC}$ of $q=8$ isocharged sequence ions F^{8+}, Ne^{8+}, Ar^{8+}, and Ca^{8+} with helium collisions at $0.4v_0$. F^{8+} was measured two times to confirm the system reproducibility. The cross-section ratio $\sigma^{DET}/\sigma^{SEC}$ varies from 0.19 (Ar^{8+}) to about 0.56 (Ne^{8+}) with the arithmetic average 0.27. This result is systematically smaller than the predictions of ECBM, MCBM, and SSL, which are 0.71, 0.63, and 0.41, respectively. In Fig. 4, the cross-section ratio $\sigma^{DET}/\sigma^{SEC}$ of the $q=9$ isocharged sequence ions F^{9+}, Ne^{9+}, Si^{9+}, S^{9+}, Ar^{9+}, and

TABLE II. Experimental cross-section ratios $\sigma^{DET}/\sigma^{SEC}$ and $\sigma^{TDC}/\sigma^{DET}$ of the $q=6$, 7, 8, 9, and 11 isocharged sequence ions collision with helium.

$q=6$ isocharged sequence									
Projectile	C^{6+}	N^{6+}	O^{6+}	F^{6+}		Ne^{6+}		Ar^{6+}	Ca^{6+}
Configuration	Bare ion	$1s^1$	$1s^2$	$1s^22s^1$		$1s^22s^2$		$[Ne]3s^2$	$[Ne]3s^23p^2$
Energy (keV/u)	6	6	6	6	3	6	3	3	3
Velocity (v_0)	0.49	0.49	0.49	0.49	0.35	0.49	0.35	0.35	0.35
$\sigma^{DET}/\sigma^{SEC}$	0.076±0.02	0.08±0.02	0.082±0.02	0.059±0.03	0.061±0.02	0.049±0.02	0.076±0.03	0.31±0.05	0.12±0.03
$\sigma^{TDC}/\sigma^{DET}$	(32±10)%	(20±10)%	(68±10)%	(38±15)%	(42±12)%	(16±8)%	(13±7)%	(97±9)%	(90±10)%
$q=7$ isocharged sequence									
Projectile	F^{7+}		Ne^{7+}	S^{7+}		Ar^{7+}		Ca^{7+}	
Configuration	$1s^2$		$1s^22s^1$	$1s^22s^22p^5$		$[Ne]3s^1$		$[Ne]3s^23p^1$	
Energy (keV/u)	4.67		4.67	4.67		4.38		3.99	
Velocity (v_0)	0.43		0.43	0.43		0.42		0.40	
$\sigma^{DET}/\sigma^{SEC}$	0.24±0.04		0.31±0.05	0.36±0.05		0.27±0.04		0.19±0.03	
$\sigma^{TDC}/\sigma^{DET}$	(5±2)%		(2±2)%	(9±3)%		(94±10)%		(90±14)%	
$q=8$ isocharged sequence									
Projectile	F^{8+}			Ne^{8+}		Ar^{8+}		Ca^{8+}	
Configuration	$1s^1$			$1s^2$		[Ne]		$[Ne]3s^2$	
Energy (keV/u)	4			4		4		4	
Velocity (v_0)	0.4			0.4		0.4		0.4	
$\sigma^{DET}/\sigma^{SEC}$	0.35±0.03		0.33±0.03	0.56±0.04		0.19±0.02		0.27±0.03	
$\sigma^{TDC}/\sigma^{DET}$	(4.3±3)%		(4.2±3)%	(4.1±4)%		(85±12)%		(82±12)%	
$q=9$ isocharged sequence									
Projectile	F^{9+}	Ne^{9+}	Si^{9+}	S^{9+}		Ar^{9+}		Ca^{9+}	
Configuration	Bare	$1s^1$	$1s^22s^22p^1$	$1s^22s^22p^3$		$1s^22s^22p^5$		$[Ne]1s^1$	
Energy (keV/u)	4.5	4.5	4.5	4.5		4.5		4.5	
Velocity (v_0)	0.42	0.42	0.42	0.42		0.42		0.42	
$\sigma^{DET}/\sigma^{SEC}$	0.19±0.02	0.16±0.02	0.32±0.03	0.25±0.03		0.26±0.03	0.25±0.03	0.21±0.03	
$\sigma^{TDC}/\sigma^{DET}$	(24±6)%	(6.8±3)%	(4±3)%	(13±8)%		(16±8)%	(16±8)%	(29±6)%	
$q=11$ isocharged sequence									
Projectile	Si^{11+}			Ar^{11+}				Ca^{11+}	
Configuration	$1s^22s^1$			$1s^22s^22p^3$				$1s^22s^22p^5$	
Energy (keV/u)	5.5			5.5				5.5	
Velocity (v_0)	0.47			0.47				0.47	
$\sigma^{DET}/\sigma^{SEC}$	0.45±0.04		0.53±0.06	0.49±0.06		0.47±0.06		0.40±0.05	
$\sigma^{TDC}/\sigma^{DET}$	(11±5)%		(9.8±7)%	(11±7)%		(6±5)%		(5.5±5)%	

Ca^{9+} collision with helium are illustrated. For F^{9+} and Ne^{9+}, the cross-section ratio $\sigma^{DET}/\sigma^{SEC}$ is about 0.16 to 0.19, but for Si^{9+}, this value is up to about 0.32. The arithmetic average of experimental data is 0.24. The experimental results are obviously under the prediction of ECBM (0.71) and MCBM (0.65), and also smaller than SSL prediction (0.41). For $q=11$ isocharged sequence ions Si^{11+}, Ar^{11+}, and Ca^{11+} collision with helium, the cross-section ratio $\sigma^{DET}/\sigma^{SEC}$ is shown in Fig. 5. The experimental values are between 0.4 and 0.53, and the arithmetic average is 0.47. The prediction of MCBM, ECBM, and SSL is 0.69, 0.72, and 0.41, respectively.

According to these figures, it seems that the projectile core factor fades away when the charge state q becomes sufficiently high. One example is the $q=11$ isocharged sequence, another is the C^{6+}, N^{6+}, O^{6+}, F^{6+}, and Ne^{6+} ions in the $q=6$ isocharged sequence. The F^{9+} and Ne^{9+} also give an instance. The first possible cause of this characteristic is that when the charge state q is sufficiently high, the projectile electrons are inert due to the high excitation energy. Second, considering that the energy of the target electrons E_e is −39.5 eV in average, therefore, the higher the projectile charge state q, the higher the states in which the transferred electrons will reside [the principal quantum number $n \approx q\sqrt{-E_e/13.6\ (\mathrm{eV})}$]. The vacant level structure of the high states are always similar for the same q.

The present results show that the cross-section ratio $\sigma^{DET}/\sigma^{SEC}$ of different ions in an isocharged sequence is not

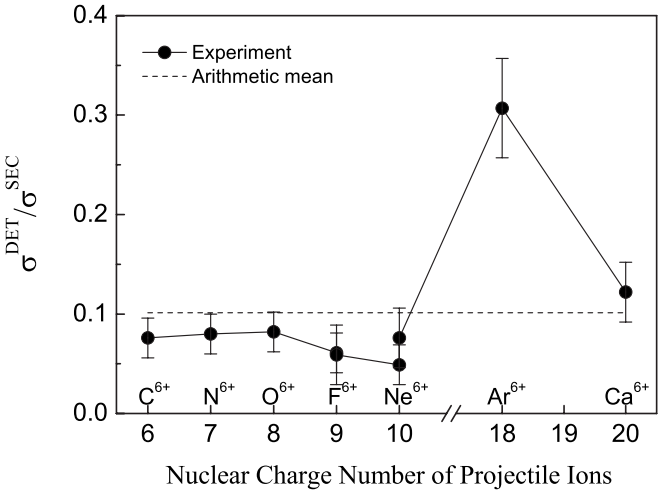

FIG. 1. Cross-section ratio $\sigma^{DET}/\sigma^{SEC}$ of the $q=6$ isocharged sequence ions collision with helium. The velocity of C^{6+}, N^{6+}, and O^{6+} is $0.49v_0$ (6 keV/u), the velocity of Ar^{6+} and Ca^{6+} is $0.35v_0$ (3 keV/u), and for F^{6+} and Ne^{6+} both velocities were measured. The cross-section ratio difference induced by different velocities is small and within present experiment uncertainties. The prediction of MCBM, ECBM, and SSL is 0.54, 0.68, and 0.41, respectively.

a constant number but varies dramatically. Our method excludes the collision velocity as a possible reason and explicitly presents the influence of the projectile-ion core properties. It implies that the projectile core strongly affects the initial electron-transfer process. During the ion-atom interaction, the transferred electrons often populate on the excited states rather than the ground state of the projectile ion. Accordingly, it is the energy of the *vacant* levels of the projectile that determines the electron-transfer efficiency.

The cross-section ratio $\sigma^{DET}/\sigma^{SEC}$ is rather independent of the collision velocity in the keV/u region [4,48,49]. The present experimental data and the data of Xe^{q+}-He ($11 \leq q \leq 31$) collision at $4q$ keV by Andersson *et al.* [6], Xe^{q+}-He

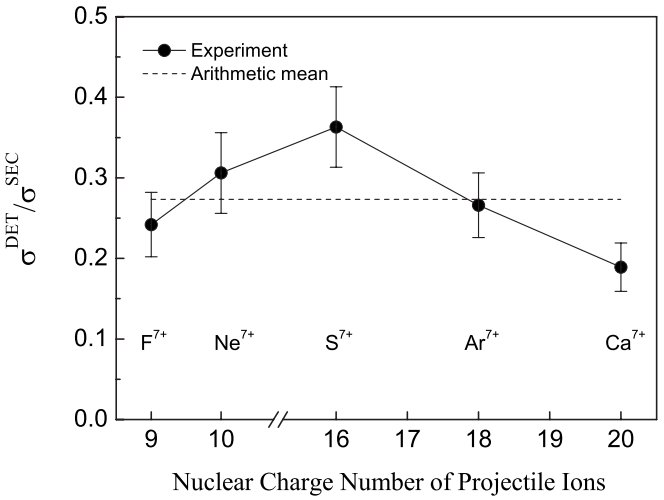

FIG. 2. Cross-section ratio $\sigma^{DET}/\sigma^{SEC}$ of the $q=7$ isocharged sequence ions F^{7+}, Ne^{7+}, S^{7+}, Ar^{7+}, and Ca^{7+} collision with helium. The collision velocity is $0.43v_0$ for all ions. The prediction of MCBM, ECBM, and SSL is 0.59, 0.70, and 0.41, respectively.

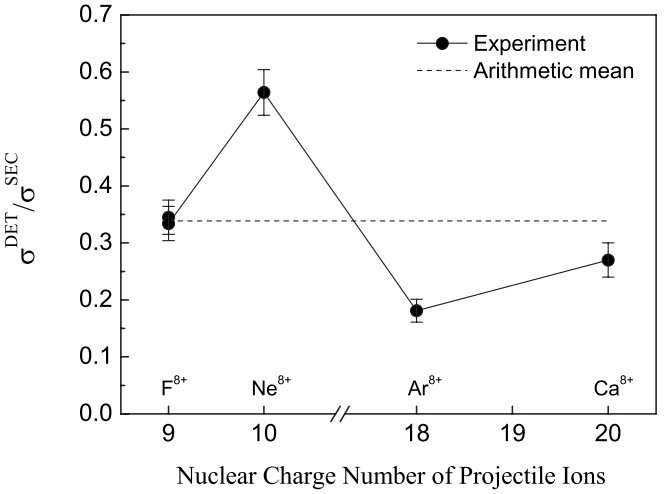

FIG. 3. Cross-section ratio $\sigma^{DET}/\sigma^{SEC}$ of the $q=8$ isocharged sequence ions F^{8+}, Ne^{8+}, Ar^{8+}, and Ca^{8+} collision with helium. The collision velocity is $0.4v_0$ for all ions. F^{8+} was measured two times to conform to system reproducibility. The prediction of MCBM, ECBM, and SSL is 0.63, 0.71, and 0.41, respectively.

($30 \leq q \leq 42$) collision at $3.8q$ keV by Selberg *et al.* [14], and Ta^{q+}-He ($41 \leq q \leq 49$) collisions at $0.3v_0$ by Madzunkov *et al.* [15] are plotted in Fig. 6. According to this figure, the cross-section ratio $\sigma^{DET}/\sigma^{SEC}$ increases averagely with the increases of q in the lower charge-state region ($q < 12$). In the higher charge-state region, this ratio remains stable except for a few points. However, the projectile core dependence is not clear in the very high charge-state region due to the lack of comparable experimental data. MCBM gives an averagely right trend but systematically overestimates the DET process, while SSL, which was generated by fitting to the data of high charge states becomes obscure when $q < 10$.

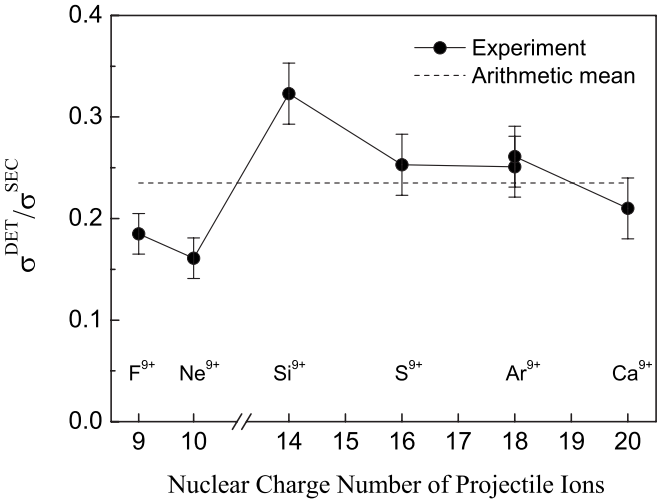

FIG. 4. Cross-section ratio $\sigma^{DET}/\sigma^{SEC}$ of the $q=9$ isocharged sequence ions F^{9+}, Ne^{9+}, Si^{9+}, S^{9+}, Ar^{9+}, and Ca^{9+} collision with helium. The collision velocity is $0.42v_0$ for all ions. Ar^{9+} was measured two times to test system reproducibility. The prediction of MCBM, ECBM, and SSL is 0.65, 0.71, and 0.41, respectively.

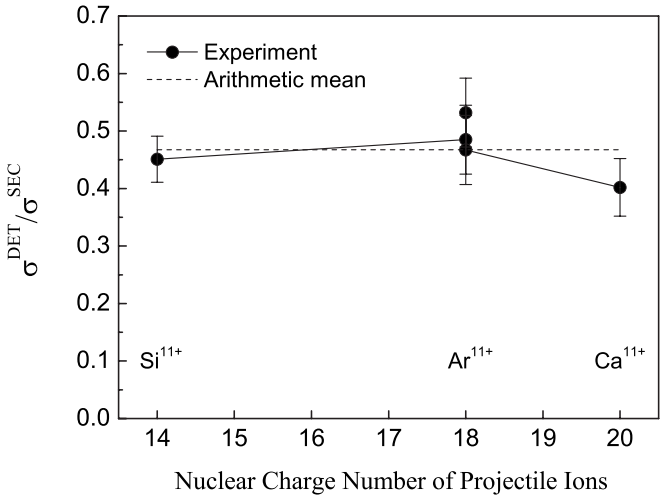

FIG. 5. Cross-section ratio $\sigma^{DET}/\sigma^{SEC}$ of the $q=11$ isocharged sequence ions Si^{11+}, Ar^{11+}, and Ca^{11+} collision with helium. The collision velocity is $0.47v_0$ for all ions. Ar^{11+} was measured three times to test system reproducibility. The prediction of MCBM, ECBM, and SSL is 0.69, 0.72, and 0.41, respectively.

Either ECBM or MCBM gives higher prediction values than the experiment. The similar phenomena were found and attributed to the TE process [10,43–47]. In addition, the experimental Q values for the TI channel were found substantially higher than the minimum Q values predicted by ECBM in Xe^{q+}-He $(25 \leq q \leq 44)$ collisions by Cederquist *et al.* [9]. They argued that this experimental result is consistent with the anomalous weakness of the DET channel and should also be attributed to the TE process. By including the TE process into ECBM, Cederquist *et al.* [10,43] investigated slow

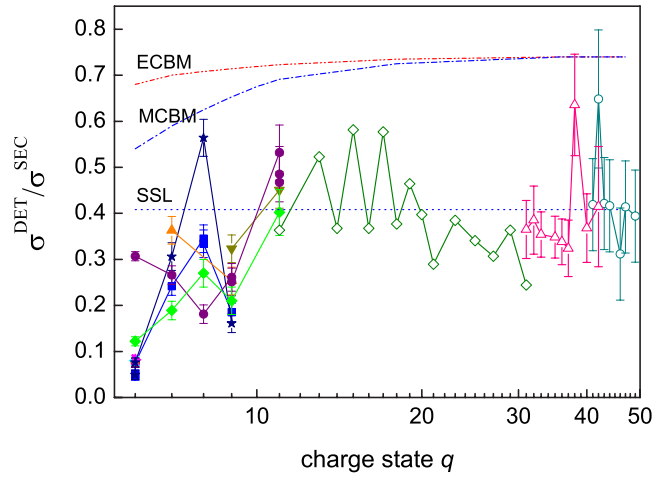

FIG. 6. (Color online) The relation between cross-section ratio $\sigma^{DET}/\sigma^{SEC}$ and charge state q. Data from this work are presented by solid symbols (● represents C^{6+} and Ar^{q+}, ♦ represents Ca^{q+}, ■ represents F^{q+}, ★ represents Ne^{q+}, ▲ represents S^{q+}, ▼ represents Si^{q+}, ◀ represents N^{6+}, and ▶ represents O^{6+}). ◇ represents the Xe^{q+}-He $(11 \leq q \leq 31)$ collision at $4q$ keV by Andersson *et al.* [6], △ represents the Xe^{q+}-He $(30 \leq q \leq 42)$ collision at $3.8q$ keV by Selberg *et al.* [14], and ◯ represents the Ta^{q+}-He $(41 \leq q \leq 49)$ collision at $0.3v_0$ by Madzunkov *et al.* [15].

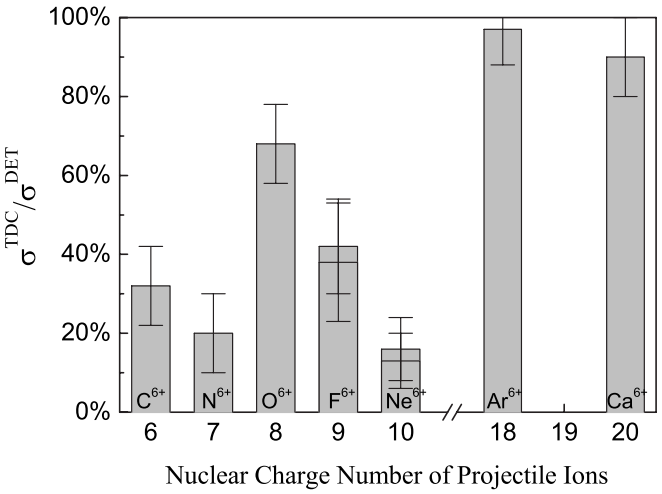

FIG. 7. Cross-section ratio $\sigma^{TDC}/\sigma^{DET}$ of the $q=6$ isocharged sequence ions collision with helium. The velocity of C^{6+}, N^{6+}, and O^{6+} is $0.49v_0$ (6 keV/u), the velocity of Ar^{6+} and Ca^{6+} is $0.35v_0$ (3 keV/u), and for F^{6+} and Ne^{6+} both velocities are measured. The cross-section ratio difference induced by different velocities is small and within present experiment uncertainties.

Xe^{q+}-He $(15 \leq q \leq 42)$ collisions and achieved better agreements with the experiments.

B. Subsequent projectile relaxation

The cross-section ratio $\sigma^{TDC}/\sigma^{DET}$ reflects the branch ratio between the radiative deexcitation and the autoionization during the projectile relaxation after the DET occurs. The cross-section ratio $\sigma^{TDC}/\sigma^{DET}$ of $q=6$, 7, 8, 9, and 11 isocharged sequence ions colliding with helium are illustrated in Figs. 7–11, respectively. The projectile ions and the experimental conditions are described in detail in the last section. Although the cross-section ratio $\sigma^{TDC}/\sigma^{DET}$ was found to be influenced by the collision velocity [29,50], in the present

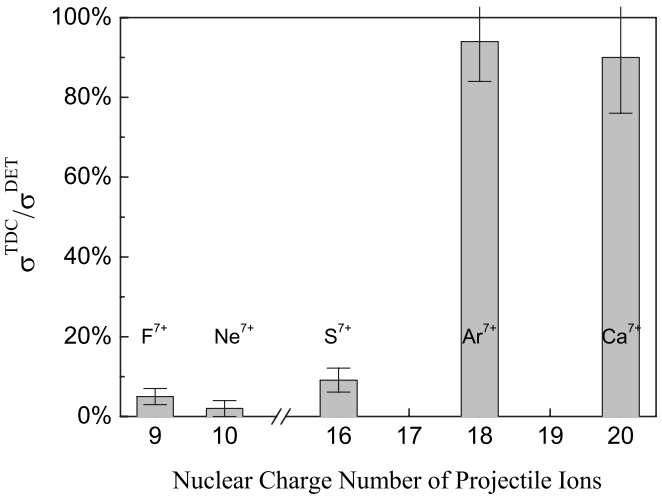

FIG. 8. Cross-section ratio $\sigma^{TDC}/\sigma^{DET}$ of the $q=7$ isocharged sequence ions F^{7+}, Ne^{7+}, S^{7+}, Ar^{7+}, and Ca^{7+} collision with helium. The collision velocity is $0.43v_0$ for all ions.

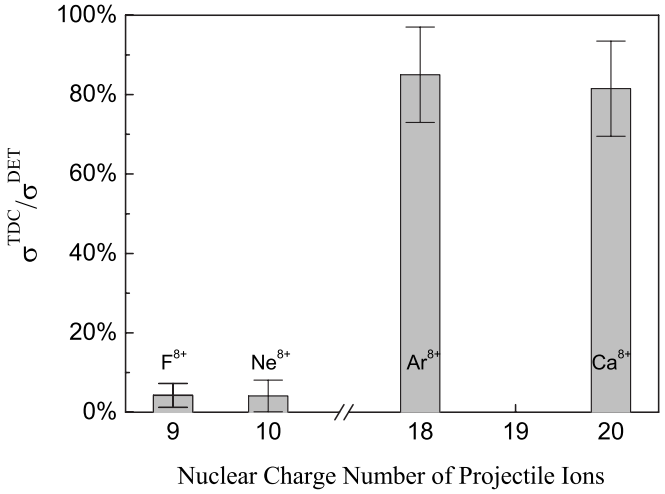

FIG. 9. Cross-section ratio $\sigma^{TDC}/\sigma^{DET}$ of the $q=8$ isocharged sequence ions F^{8+}, Ne^{8+}, Ar^{8+}, and Ca^{8+} collision with helium. The collision velocity is $0.4v_0$ for all ions. F^{8+} was measured two times to confirm system reproducibility.

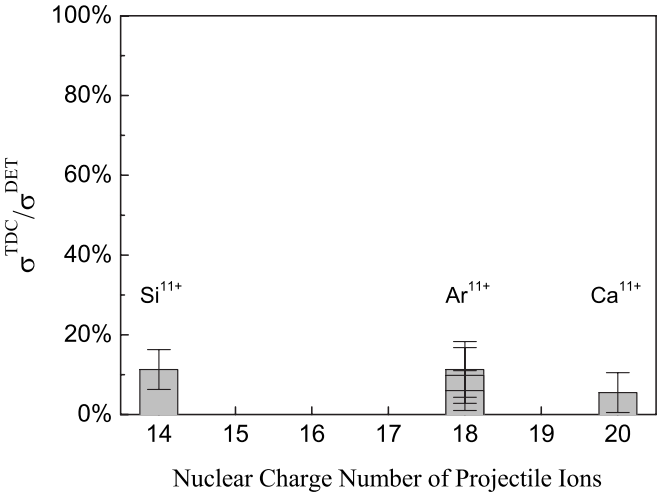

FIG. 11. Cross-section ratio $\sigma^{TDC}/\sigma^{DET}$ of the $q=11$ isocharged sequence ions Si^{11+}, Ar^{11+}, and Ca^{11+} collision with helium. The collision velocity is $0.47v_0$ for all ions. Ar^{11+} was measured three times to test system reproducibility.

cases the collision velocities were the same for an isocharged sequence, and between different sequences the difference of the velocities are also small (varies from $0.35v_0$ to $0.49v_0$).

Figure 7 shows that for C^{6+}, N^{6+}, F^{6+}, and Ne^{6+} the autoionization dominates after the DET occurs, and for Ar^{6+} and Ca^{6+}, the radiative deexcitation dominates. The similar phenomenon exists in the $q=7$ (Fig. 8) and $q=8$ (Fig. 9) isocharged sequences, i.e., the autoionization dominates for the lighter ions and the radiative deexcitation dominates for the heavier ions Ar^{q+} and Ca^{q+}. However, for the higher charge states such as $q=9$ (Fig. 10) and $q=11$ (Fig. 11) isocharged sequences, the autoionization dominates for all of the ions.

It is remarkable that the radiative deexcitation is close to unity for $Ar^{6,7,8+}$ and $Ca^{6,7,8+}$. For these relative lowly charged ions, the vacant energy levels are very closely spaced allowing for resonant electron transfer. In addition, due to the lower excitation energy, the projectile electrons could also be excited during the ion-atom interaction. Therefore, after the DET occurs, the two transferred electrons may rather reside in different principal shells than in the same principal shell. The intershell electron-electron interaction is weaker, and consequently, autoionizing decay is less likely. Also, for these low-charge ions excitation energies may not be enough to allow for autoionizing decay. Oppositely, for the highly charged lighter ions such as F^{q+} and Ne^{q+} ($q=7$, 8 and 9), radiative deexcitation is rather weak and autoionization dominates, because autoionization is energetically well possible. In addition, the relevant energy levels of these lighter ions are sparser, and because the ionization potential difference of the two electrons is smaller than the difference of the vacant levels of the projectile ions, the two electrons are often captured into symmetrical states. The inner-shell electron-electron interaction is strong, which tends to further promote autoionization.

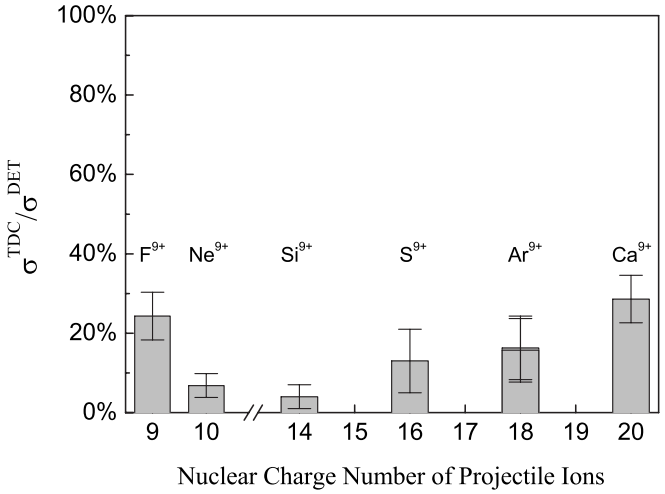

FIG. 10. Cross-section ratio $\sigma^{TDC}/\sigma^{DET}$ of the $q=9$ isocharged sequence ions F^{9+}, Ne^{9+}, Si^{9+}, S^{9+}, Ar^{9+}, and Ca^{9+} collision with helium. The collision velocity is $0.42v_0$ for all ions. Ar^{9+} was measured two times to test system reproducibility.

The data of the Xe^{q+}-He ($11 \leq q \leq 31$) collision at $4q$ keV by Andersson *et al.* [6] and the Xe^{q+}-He ($30 \leq q \leq 42$) collision at $3.8q$ keV by Selberg *et al.* [14] and the present data are plotted in Fig. 12 together. According to Figs. 10–12, it can be seen that generally the autoionization is dominant in the higher charge-state region, although the agreement between the experimental results of Andersson *et al.* and Selberg *et al.* is not perfect. As the charge state becomes sufficiently high, the projectile electrons become inert, and the vacant level structure of the ions becomes homologous. On the other hand, the target electron-HCI interaction becomes stronger. When the electron-HCI interaction overwhelms the electron-electron interaction, the one-step mechanism may be magnified. In this situation, the two target electrons could be transferred simultaneously with the same energy, and then be populated symmetrically. Consequently, the electron-electron interaction is strong and the autoionization deexcitation dominates during the projectile relaxation.

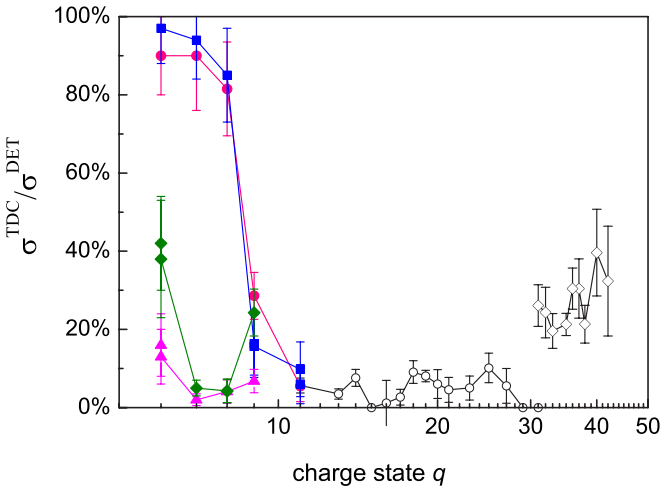

FIG. 12. (Color online) The relation between cross-section ratio $\sigma^{TDC}/\sigma^{DET}$ and charge state q. Data from this work are presented by solid symbols. ◯ represents the Xe^{q+}-He $(11 \leq q \leq 31)$ collision at $4q$ keV by Andersson *et al.* [6] and ◇ represents the Xe^{q+}-He $(30 \leq q \leq 42)$ collision at $3.8q$ keV by Selberg *et al.* [14].

V. CONCLUSIONS

The isocharged sequence ions with helium collisions were investigated in the keV/u region. The cross-section ratio $\sigma^{DET}/\sigma^{SEC}$ indicates the electrons repopulation during the ion-atom interaction. The cross-section ratio $\sigma^{TDC}/\sigma^{DET}$ represents the relative percentage of the radiative deexcitation to the DET process, which indicates the electron-electron interaction during the projectile relaxation. This work shows that both the cross-section ratios $\sigma^{DET}/\sigma^{SEC}$ and $\sigma^{TDC}/\sigma^{DET}$ are strongly affected by the projectile-ion core properties, which suggests that the projectile core strongly affects both the initial electron transfer and the subsequent projectile relaxation.

For different ions in an isocharged sequence, the cross-section ratio $\sigma^{DET}/\sigma^{SEC}$ varies by a factor of 3. Moreover, in terms of the arithmetic average of the experimental data, MCBM gives a roughly right trend but systematically overestimates the DET process, and SSL gives better estimations when $q > 10$. ECBM, MCBM, and SSL severely overestimate the DET process for those lower charge-state sequences. However, the classical over-the-barrier models and the semiempirical scaling laws describe the projectile ion with only one parameter, i.e., its charge state q, and therefore cannot distinguish different ions in an isocharged sequence. In addition, only the two-step mechanism is considered in ECBM and MCBM for the DET process; the one-step mechanism as well as the transfer excitation are neglected. The present work shows that this simplification is insufficient. To improve these intuitional models, the projectile-ion core properties, the simultaneous capture mechanism, and the transfer excitation should be appropriately considered.

The cross-section ratio $\sigma^{TDC}/\sigma^{DET}$ is substantially determined by the double-electron population scheme, which is originated from the vacant energy level structure of the projectile ions. For those lowly charged ions, the projectile-ion core properties dramatically affect the experimental cross-section ratio $\sigma^{TDC}/\sigma^{DET}$. And for those sufficiently charged ions, the electrons are populated on the high-level states and the projectile core becomes unimportant, therefore the autoionization always dominates during the post-collision interaction.

ACKNOWLEDGMENTS

We thank the staff of the ECRIS group of the Institute of Modern Physics, Chinese Academy of Sciences, for their help on the running of the ECRIS. This work was supported by the National Natural Science Foundation of China under Grants No. 10304019, No. 10134010, and No. 10375080.

[1] R. K. Janev and H. Winter, Phys. Rep. **117**, 265 (1985).
[2] W. Fritsch and C. D. Lin, Phys. Rep. **202**, 1 (1991).
[3] R. K. Janev and L. P. Presnyakov, Phys. Rep. **70**, 1 (1981).
[4] M. Barat and P. Roncin, J. Phys. B **25**, 2205 (1992).
[5] E. Justiniano, C. L. Cocke, T. J. Gray, R. Dubois, C. Can, W. Waggoner, R. Schuch, H. Schmidt-Böcking, and H. Ingwersen, Phys. Rev. A **29**, 1088 (1984).
[6] H. Andersson, G. Astner, and H. Cederquist, J. Phys. B **21**, L187 (1988).
[7] J. Vancura, V. J. Marchetti, J. J. Perotti, and V. O. Kostroun, Phys. Rev. A **47**, 3758 (1993).
[8] H. Cederquist, C. Biedermann, N. Selberg, and P. Hvelplund, Phys. Rev. A **51**, 2169 (1995).
[9] H. Cederquist, C. Biedermann, N. Selberg, and P. Hvelplund, Phys. Rev. A **51**, 2191 (1995).
[10] H. Cederquist, Phys. Rev. A **43**, 2306 (1991).
[11] X. Fléchard, C. Harel, H. Jouin, B. Pons, L. Adoui, F. Frémont, A. Cassimi, and D. Hennecart, J. Phys. B **34**, 2759 (2001).
[12] S. Bliman, R. Bruch, M. Cornille, A. Langereis, and J. Nordgren, Phys. Rev. A **66**, 052707 (2002).
[13] N. Selberg, C. Biedermann, and H. Cederquist, Phys. Rev. A **54**, 4127 (1996).
[14] N. Selberg, C. Biedermann, and H. Cederquist, Phys. Rev. A **56**, 4623 (1997).
[15] S. Madzunkov, D. Fry, and R. Schuch, J. Phys. B **37**, 3239 (2004).
[16] W. Fritsch and C. D. Lin, J. Phys. B **19**, 2683 (1986).
[17] W. Fritsch and C. D. Lin, Phys. Rev. A **45**, 6411 (1992).
[18] W. Fritsch and C. D. Lin, Phys. Rev. A **54**, 4931 (1996).
[19] M. C. Bacchus-Montabonel, Phys. Rev. A **53**, 3667 (1996).
[20] C. Chaudhuri, S. Sanyal, and T. K. Rai Dastidar, Phys. Rev. A **52**, 1137 (1995).
[21] Y. S. Tergiman and M. C. Bacchus-Montabonel, Phys. Rev. A **64**, 042721 (2001).
[22] I. Y. Tolstikhina, O. I. Tolstikhin, and H. Tawara, Phys. Rev. A **57**, 4387 (1998).
[23] H. Knudsen, H. K. Haugen, and P. Hvelplund, Phys. Rev. A **23**, 597 (1981).

[24] A. Bárány, G. Astner, H. Cederquist, H. Danared, S. Huldt, P. Hvelplund, A. Johnson, H. Knudsen, L. Liljeby, and K.-G. Rensfelt, Nucl. Instrum. Methods Phys. Res. B **9**, 397 (1985).
[25] A. Niehaus, J. Phys. B **19**, 2925 (1986).
[26] F. Frémont, C. Bedouet, X. Husson, and J.-Y. Chesnel, Phys. Rev. A **57**, 4379 (1998).
[27] M. Schulz, R. Moshammer, D. Fischer, H. Kollmus, D. H. Madison, S. Jones, and J. Ullrich, Nature **422**, 48 (2003).
[28] J.-Y. Chesnel, B. Sulik, H. Merabet, C. Bedouet, F. Frémont, X. Husson, M. Grether, A. Spieler, and N. Stolterfoht, Phys. Rev. A **57**, 3546 (1998).
[29] J.-Y. Chesnel, H. Merabet, B. Sulik, F. Frémont, C. Bedouet, X. Husson, M. Grether, and N. Stolterfoht, Phys. Rev. A **58**, 2935 (1998).
[30] E. Y. Kamber, M. A. Abdallah, C. L. Cocke, and M. Stöckli, Phys. Rev. A **60**, 2907 (1999).
[31] D. Dijkkamp, Y. S. Gordeev, A. Brazuk, A. G. Drentje, and F. J. de Heer, J. Phys. B **18**, 737 (1985).
[32] J. P. M. Beijers, R. Hoekstra, A. R. Schlatmann, R. Morgenstern, and F. J. de Heer, J. Phys. B **25**, 463 (1992).
[33] J. P. M. Beijers, R. Hoekstra, R. Morgenstern, and F. J. de Heer, J. Phys. B **25**, 4851 (1992).
[34] G. de Nijs, H. O. Folkerts, R. Hoekstra, and R. Morgenstern, J. Phys. B **29**, 85 (1996).
[35] X. Cai, D. Yu, R. Lu, Z. Cao, W. Yang, C. Shao, X. Chen, and X. Ma, Nucl. Instrum. Methods Phys. Res. B **225**, 185 (2004).
[36] X. Cai, D. Yu, Z. Cao, R. Lu, W. Yang, C. Shao, and X. Chen, Chin. Phys. **13**, 1679 (2004).
[37] J. Bernard, R. Brédy, S. Martin, L. Chen, J. Désesquelles, and M. C. Buchet-Poulizac, Phys. Rev. A **66**, 013209 (2002).
[38] N. Bohr and J. Lindhardt, K. Dan. Vidensk. Selsk. Mat. Fys. Medd. **28**, No. 7 (1954).
[39] H. Ryufuku, K. Sasaki, and T. Watanabe, Phys. Rev. A **21**, 745 (1980).
[40] L. Guillemot, P. Roncin, M. N. Gaboriaud, H. Laurent, and M. Barat, J. Phys. B **23**, 4293 (1990).
[41] N. Nakamura, F. J. Currell, A. Danjo, M. Kimura, A. Matsumoto, S. Ohtani, H. A. Sakaue, M. Sakurai, H. Tawara, and H. Watanabe *et al.*, J. Phys. B **28**, 2959 (1995).
[42] W. Wu, C. L. Cocke, J. P. Giese, F. Melchert, M. L. A. Raphaelian, and M. Stöckli, Phys. Rev. Lett. **75**, 1054 (1995).
[43] H. Cederquist, E. Beebe, C. Biedermann, A. Engstrom, H. Gao, R. Hutton, J. C. Levin, L. Liljeby, T. Quinteros,and N. Selberg *et al.*, J. Phys. B **25**, L69 (1992).
[44] W. Fritsch, Phys. Lett. A **192**, 369 (1994).
[45] R. Parameswaran, C. P. Bhalla, B. P. Walch, and B. D. DePaola, Phys. Rev. A **43**, 5929 (1991).
[46] N. Shimakura, S. Yamada, S. Suzuki, and M. Kimura, Phys. Rev. A **51**, 2989 (1995).
[47] E. Y. Kamber, K. Akgüngör, C. Leather, and A. G. Brenton, Phys. Rev. A **54**, 1452 (1996).
[48] H. Klinger, A. Müller, and E. Salzborn, J. Phys. B **8**, 230 (1975).
[49] A. Müller, H. Klinger, and E. Salzborn, Phys. Lett. **55**, 11 (1975).
[50] D. Yu, X. Cai, R. Lu, C. Shao, J. Lu, F. Ruan, H. Zhang, Y. Cui, X. Xu, and J. Shao *et al.*, Chin. Phys. Lett. **22**, 1398 (2005).